76-6

GRAIN BOUNDARY DISLOCATIONS IN NONCUBIC CRYSTALS - I. THE MODEL

GORDON A. BRUGGEMAN and GEORGE H. BISHOP, Jr.
MATERIALS SCIENCES DIVISION

March 1976

ARMY MATERIALS AND MECHANICS RESEARCH CENTER
Watertown, Massachusetts 02172

The findings in this report are not to be construed as an official Department of the Army position, unless so designated by other authorized documents.

Mention of any trade names or manufacturers in this report shall not be construed as advertising nor as an official indorsement or approval of such products or companies by the United States Government.

DISPOSITION INSTRUCTIONS

Destroy this report when it is no longer needed.
Do not return it to the originator.

DISCLAIMER NOTICE

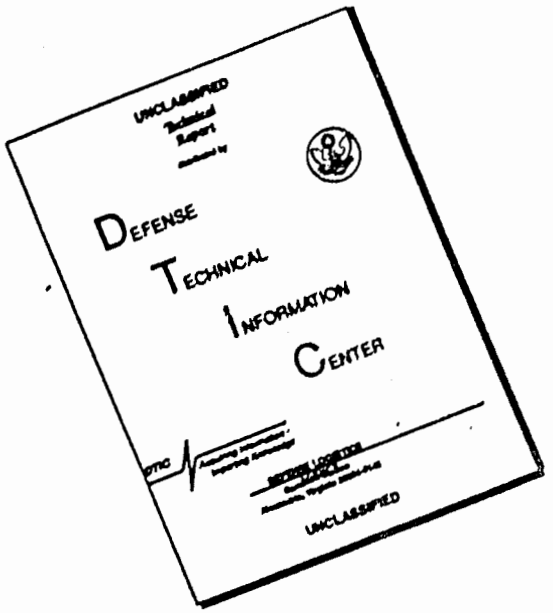

THIS DOCUMENT IS BEST QUALITY AVAILABLE. THE COPY FURNISHED TO DTIC CONTAINED A SIGNIFICANT NUMBER OF PAGES WHICH DO NOT REPRODUCE LEGIBLY.

UNCLASSIFIED

SECURITY CLASSIFICATION OF THIS PAGE (When Date Entered)

REPORT DOCUMENTATION PAGE

READ INSTRUCTIONS BEFORE COMPLETING FORM

1. REPORT NUMBER: AMMRC TR 76-6	2. GOVT ACCESSION NO.
3. RECIPIENT'S CATALOG NUMBER	
4. TITLE (and Subtitle): GRAIN BOUNDARY DISLOCATIONS IN NONCUBIC CRYSTALS — I. THE MODEL	5. TYPE OF REPORT & PERIOD COVERED: Final Report
6. PERFORMING ORG. REPORT NUMBER	
7. AUTHOR(s): Gordon A. Bruggeman and George H. Bishop, Jr.	8. CONTRACT OR GRANT NUMBER(s)
9. PERFORMING ORGANIZATION NAME AND ADDRESS: Army Materials and Mechanics Research Center, Watertown, Massachusetts 02172, DRXMR-D	10. PROGRAM ELEMENT, PROJECT, TASK AREA & WORK UNIT NUMBERS: D/A Project: 1T161102B32A; AMCMS Code: 611102.11.85500; Agency Accession: DA 0D4767
11. CONTROLLING OFFICE NAME AND ADDRESS: U. S. Army Materiel Development and Readiness Command, Alexandria, Virginia 22333	12. REPORT DATE: March 1976
	13. NUMBER OF PAGES: 21
14. MONITORING AGENCY NAME & ADDRESS (if different from Controlling Office)	15. SECURITY CLASS. (of this report): Unclassified
	15a. DECLASSIFICATION/DOWNGRADING SCHEDULE

16. DISTRIBUTION STATEMENT (of this Report)

Approved for public release; distribution unlimited.

17. DISTRIBUTION STATEMENT (of the abstract entered in Block 20, if different from Report)

18. SUPPLEMENTARY NOTES

19. KEY WORDS (Continue on reverse side if necessary and identify by block number)

Grain boundaries	Zinc	Crystal structure
Crystallography	Interfaces	
Dislocations	Crystal defects	
Topology	Models	

20. ABSTRACT (Continue on reverse side if necessary and identify by block number)

(SEE REVERSE SIDE)

DD FORM 1 JAN 73 1473 EDITION OF 1 NOV 65 IS OBSOLETE

UNCLASSIFIED

SECURITY CLASSIFICATION OF THIS PAGE (When Date Entered)

Block No. 20

ABSTRACT

A model is developed for the dislocation structure of grain boundaries in noncubic crystals. Important differences are noted between the grain boundary dislocation (GBD) description of boundaries in cubic and noncubic crystals. In both types of crystals the GBD's are present to preserve low-energy patterns characteristic of exact coincidence-site lattices (CSL's). In cubic crystals exact three-dimensional CSL's can be found for rotations about any axis. In noncubic crystals, however, exact three-dimensional CSL's exist only in special circumstances; in general, only near-coincidence site lattices (near-CSL's) can occur in three dimensions. When only near-coincidence is possible an additional component to the GBD array is necessary to compensate for the distortion implicit in near-coincidence. In twist boundaries this additional component alters the spacing of dislocations in the screw grid. Moreover, it is impossible to obtain a twist boundary free of GBD's. The minimum dislocation content occurs at misorientations at which exact coincidence exists in a single plane parallel to the twist axis, i.e., when an exact two-dimensional CSL exists, in which case a single set of screw GBD's parallel to the plane of exact coincidence is present. In tilt boundaries two dislocation arrays may be necessary: an array of pattern-preserving dislocations and an array of misfit dislocations. The function of the former array is to preserve the low-energy coincidence pattern on either side of the GBD; the function of the misfit array is again to compensate for the distortion inherent in near-coincidence. The pattern-preserving GBD's are shown to introduce steps in tilt grain boundaries, altering the boundary inclination as the dislocation content of the boundary varies. As a result, a systematic, experimentally verifiable coupled change in boundary inclination with boundary misorientation is predicted for each potential pattern-preserving GBD.

CONTENTS

INTRODUCTION

A large number of recent experimental observations have provided irrefutable evidence that dislocations are an intrinsic part of the structure of many high-angle grain boundaries.[1-20] Such observations conform to the expectations of the coincidence model of grain boundaries[21-23] in which it has been suggested that a dislocation network will be formed whenever, for energetic reasons, the crystal tends to conserve a particular pattern of atomic sites in the boundary, where the pattern that is conserved is characteristic of a coincidence boundary of lower energy occurring at a nearby misorientation. Indeed, grain boundaries deviating slightly from coincidence misorientations have been observed to contain a network of grain boundary dislocations (GBD's) in which the dislocations delineate regions of the boundary having essentially the structure of the coincidence boundary. The mathematical basis for the description of these dislocation networks has been formally developed and generalized by Bollmann[24] in his theory of crystalline interfaces.

From the standpoint of Bollmann's geometrical development, the Burgers vector of a grain boundary dislocation must determine a lattice displacement of one

1. BOLLMANN, W., and NISSEN, H.-U. *A Study of Optimal Phase Boundaries: The Case of Exsolved Alkali Feldspars.* Acta Cryst., v. 24A, 1968, p. 546-557.
2. GLEITER, H., HORNBOGEN, E., and BARO, G. *The Mechanism of Grain Boundary Glide.* Acta Met., v. 16, 1968, p. 1053-1067.
3. ISHIDA, Y., HASEGAWA, T., and NAGATA, F. *Grain-Boundary Fine Structure in an Iron Alloy.* J. Appl. Phys., v. 40, 1969, p. 2182-2186.
4. LEVY, J. *The Structure of High-Angle Grain Boundaries in Aluminum.* Phys. Stat. Sol., v. 31, 1969, p. 193-201.
5. SCHOBER, T., and BALLUFFI, R. W. *Dislocation Subboundary Arrays in Oriented Thin-Film Bicrystals.* Phil. Mag., v. 20, 1969, p. 511-518.
6. GLEITER, H. *The Mechanism of Grain Boundary Migration.* Acta Met., v. 17, 1969, p. 565-573.
7. SCHOBER, T., and BALLUFFI, R. W. *Quantitative Observation of Misfit Dislocation Arrays in Low and High-Angle Twist Grain Boundaries.* Phil. Mag., v. 21, 1970, p. 109-123.
8. SCHOBER, T. *Observation of Misfit Dislocation Arrays in High Angle (110) Twist Grain Boundaries in Gold.* Phil. Mag., v. 22, 1970, p. 1063-1068.
9. SCHOBER, T., and BALLUFFI, R. W. *Extraneous Grain Boundary Dislocations in Low and High Angle (001) Twist Boundaries in Gold.* Phil. Mag., v. 24, 1971, p. 165-180.
10. SCHOBER, T., and BALLUFFI, R. W. *Observation of Dislocation Arrays in Low Angle Tilt Boundaries in Gold.* Phys. Stat. Sol. (b), v. 44, 1971, p. 103-114.
11. SCHOBER, T., and BALLUFFI, R. W. *Dislocations in Symmetric High Angle [001] Tilt Boundaries in Gold.* Phys. Stat. Sol. (b), v. 44, 1971, p. 115-126.
12. BUZZICHELLI, G., and MASCANZONI, A. *On the Generation and Motion of Grain Boundary Dislocations in Steel.* Phil. Mag., v. 24, 1971, p. 497-508.
13. BALLUFFI, R. W., WOOLHOUSE, G. R., and KOMEN, Y. *On Grain Boundary Dislocation Contrast in the Electron Microscope* in The Nature and Behavior of Grain Boundaries, H. Hu, ed., Plenum Press, 1972, p. 41.
14. BALLUFFI, R. W., KOMEN, Y., and SCHOBER, T. *Electron Microscope Studies of Grain Boundary Dislocation Behavior.* Surface Science, v. 31, 1972, p. 68-103.
15. MIEKK-OJA, H. M., and LINDROOS, V. K. *The Formation of Dislocation Networks.* Surface Science, v. 31, 1972, p. 422-455.
16. SCHOBER, T., and WARRINGTON, D. H. *Extraneous Grain Boundary Dislocations in High Angle (110) Twist Boundaries in Gold.* Phys. Stat. Sol. (a), v. 6, 1971, p. 103-110.
17. BALLUFFI, R. W., SASS, S. L., and SCHOBER, T. *Grain Boundary Dislocation Networks as Electron Diffraction Gratings.* Phil. Mag., v. 26, 1972, p. 585-592.
18. LOBERG, B., and NORDEN, H. *Regular Defect Structures in High Angle Grain Boundaries.* Acta Met., v. 21, 1973, p. 213-218.
19. KEGG, G. R., HORTON, C. A. P., and SILCOCK, J. M. *Grain Boundary Dislocations in Aluminum Bicrystals After High-Temperature Deformation.* Phil. Mag., v. 27, no. 5, May 1973, p. 1041-1055.
20. McDONALD, R. C., and ARDELL, A. J. *On Diffraction Contrast Effects at Extrinsic Grain Boundary Dislocations.* Phys. Stat. Sol. (a), v. 18, 1973, p. 407-417.
21. BRANDON, D. G., RALPH, B., RANGANATHAN, S., and WALD, M. S. *A Field Ion Microscope Study of Atomic Configuration at Grain Boundaries.* Acta Met., v. 12, 1964, p. 813-821.
22. BRANDON, D. G. *The Structure of High-Angle Grain Boundaries.* Acta Met., v. 14, 1966, p. 1479-1484.
23. BISHOP, G. H., and CHALMERS, B. *A Coincidence-Ledge-Dislocation Description of Grain Boundaries.* Scripta Met., v. 2, 1968, p. 133-140.
24. BOLLMANN, W. *Crystal Defects and Crystalline Interfaces.* Springer-Verlag, 1970, p. 148.

crystal relative to the other which allows the same pattern of atomic sites to be preserved in the boundary on both sides of the dislocation. In low-angle boundaries, where the pattern of sites preserved on both sides of the dislocation is characteristic of the perfect crystal, the only permissible displacements are real lattice vectors and the grain boundary dislocations are simple lattice dislocations. In high-angle boundaries, however, where the pattern of boundary sites may be characteristic of a high-angle coincidence misorientation, the pattern-preserving displacements are usually not equal to lattice vectors, but instead are given by vectors within Bollmann's "complete-pattern-shift" lattice or DSC lattice. Hence the Burgers vectors of dislocations in high-angle grain boundaries will equal DSC lattice vectors and so will tend to be different from real lattice vectors, consistent with most experimental observations. Hirth and Balluffi[25] have discussed various crystallographic aspects of these grain boundary dislocations, distinguishing between several types of GBD's.

An alternate but equivalent view of the structure of high-angle grain boundaries is provided in the structural unit version of coincidence theory.[23,26,27] Simply stated, this model holds that grain boundaries are made up of mixtures of a relatively small number of structural units where the structural units are segments of coincidence or near-coincidence boundaries occurring at nearby misorientations. In a recent paper[28] this model was used by the present authors as the basis for an explanation of earlier observations of grain boundary faceting in zinc bicrystals.[29] The model was shown not only to produce excellent agreement with then-observed grain boundary facet morphologies, but also to possess predictive capabilities enabling the forecast of specific morphologies occurring at other misorientations, which were subsequently observed experimentally.

Thus far the grain boundary dislocation description of grain boundaries has not been extensively applied to noncubic crystals, nor has it been developed along a line which would relate macroscopic aspects of grain boundary morphology (such as low-energy boundary inclinations) to the dislocation structure. The microscopic equivalence of the GBD and structural unit models has been demonstrated in the simple case of symmetric tilt boundaries near coincidence misorientations in cubic crystals,[23,26] but a more general equivalence in noncubic crystals and at other boundary inclinations has not been shown, although such a general equivalence can be anticipated. In this paper we examine the modifications of the GBD model necessitated by its application to noncubic crystals and demonstrate a coupling between boundary dislocation structure and boundary inclination in asymmetric tilt boundaries. In so doing the background is laid for the use of the GBD description in an interpretation of our earlier observations of grain boundary faceting in zinc, to be presented in the subsequent paper (Part II).

25. HIRTH, J. P., and BALLUFFI, R. W. *On Grain Boundary Dislocations and Ledges.* Acta Met., v. 21, 1973, p. 929-942.
26. BISHOP, G. H., and CHALMERS, B. *Dislocation Structure and Contrast in High-Angle Grain Boundaries.* Phil. Mag., v. 24, 1971, p. 515-526.
27. BRUGGEMAN, G. A., BISHOP, G. H., and HARTT, W. H. *Coincidence and Near-Coincidence Grain Boundaries in HCP Metals* in The Nature and Behavior of Grain Boundaries, H. Hu, ed., Plenum Press, 1972, p. 83.
28. HARTT, W. H., BISHOP, G. H., and BRUGGEMAN, G. A. *Grain Boundary Faceting of $\langle 10\bar{1}0 \rangle$ Tilt Boundaries in Zinc – Part II.* Acta Met., v. 22, 1974, p. 971-983.
29. BISHOP, G. H., HARTT, W. H., and BRUGGEMAN, G. A. *Grain Boundary Faceting of $\langle 10\bar{1}0 \rangle$ Tilt Boundaries in Zinc.* Acta Met., v. 19, 1971, p. 37-47.

THE GBD MODEL — DEVIATIONS FROM EXACT COINCIDENCE MISORIENTATIONS

The structural unit model for high-angle grain boundaries begins with the premise that the structural units comprising a general grain boundary will be short segments of coincidence or near-coincidence boundaries occurring at nearby misorientations. The analogous starting point for the GBD description holds that the pattern of atomic sites preserved in the boundary on either side of a grain boundary dislocation is characteristic of a nearby exact coincidence boundary, and hence is characteristic of the pattern of sites represented by a given coincidence-site lattice (CSL). Thus in the GBD description of grain boundaries, probable low-energy patterns of boundary sites may be identified with the various CSL's and the pattern-preserving displacements or GBD Burgers vectors defined by the related DSC lattices. While every pattern-preserving displacement so defined is a crystallographically permissible Burgers vector for a GBD, there clearly are critical characteristics which must act in the selection of those few which can be associated with low-energy boundary structures.

Although coincidence has physical significance only at the interface between two crystals, it is necessary that the three-dimensional coincidence array represented by the CSL be considered in order to portray the pattern of coincidence sites potentially present in boundaries of various inclinations at the coincidence misorientation. High densities of coincidence sites will in general occur on low-index planes of the CSL, thereby defining the potential two-dimensional coincidence patterns by which the structures of coincidence boundaries may be characterized. Of course, the actual arrangement of atoms in the boundary plane cannot be precisely determined from these geometric considerations alone. Nevertheless, irrespective of what the detailed atom locations within the pattern may be, the pattern of sites will be periodically reproduced over large areas of the boundary, where the *unit of periodicity* can be defined in terms of the coincidence-site lattice. From this follows the simple but critical point that the same pattern-preserving displacements that are able to preserve the three-dimensional CSL are therefore able to also preserve the two-dimensional patterns of sites characteristic of the coincidence boundaries in their various inclinations.

Figure 1 illustrates the relationship between a CSL and its associated DSC lattice. Here two interpenetrating simple cubic lattices have been misoriented by a rotation of 53.1° about the common [010] direction to yield the $\Sigma = 5$ coincidence-site lattice. The sublattice drawn within the unit cell PQRS of the CSL is the DSC lattice for this particular array of coincidence sites. The DSC lattice may be derived analytically as described by Bollmann,[24] or alternately it may be constructed based upon the geometric property of all DSC lattices that every DSC

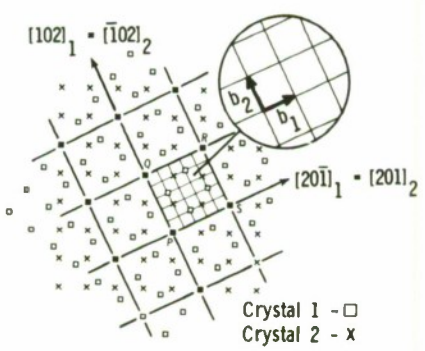

Figure 1. One (010) layer of two interpenetrating simple cubic crystals misoriented by 53.1° about the common [010] direction. The heavy lines outline the $\Sigma = 5$ coincidence-site lattice. The sublattice drawn within the unit cell PQRS is the DSC lattice for this coincidence array.

lattice vector is a difference vector between lattice points on Crystal 1 and lattice points on Crystal 2. In this case the unit vectors b_1 and b_2 of this DSC lattice are both vectors of the form 1/5<102>. The third unit vector, normal to the plane of the figure, is [010] in both crystals. Separating the two crystals by a boundary plane normal to the rotation axis results in an [010] twist boundary in which the coincidence pattern PQRS is the unit of periodicity. Similarly, a boundary plane parallel to the [010] rotation axis, having the line PQ as its trace in the (010) plane, is an [010] tilt boundary in one of three possible symmetric inclinations (PR and PS are traces of the others), where the period of the repeating coincidence pattern is given by the length PQ.

Should the two rigid crystal lattices be rotated slightly off the coincidence misorientation, say by having the misorientation about [010] slightly less than 53.1°, coincidence is destroyed and the three-dimensional CSL no longer exists; grain boundaries which were formerly coincidence boundaries would now be off-coincidence boundaries. This situation is illustrated in Figure 2. All former coincidence sites will have been displaced from one another by the slight rotation away from the coincidence misorientation, with the exception of the single row of coincidence sites which may lie along the rotation axis, e.g., the normal to point P in Figure 2a. The configuration of the coincidence pattern characteristic of Figure 1 can still be discerned near point P, but as the radial distance from P increases the coincidence pattern gradually disappears as the displacements between former coincidence sites increase. However, near those regions where the displacements between former coincidence sites are nearly equal to DSC lattice vectors, the relative crystal positions approximate what they are near point P, and the coincidence pattern can once again be discerned.

Centered on such regions in off-coincidence boundaries are areas in which coincidence can be restored by simply allowing the crystals to strain slightly to conform to the previous coincidence pattern, while localizing the mismatch between contiguous areas of this type in the cores of grain boundary dislocations. For example, in the twist boundary parallel to the plane PQ'R'S', the (presumably) low-energy coincidence pattern PQRS of Figure 1 will be preserved over large areas of the boundary by localizing the displacements between coincidence sites in the displacement fields of a crossed network of screw dislocations, as represented schematically in Figure 2b. The actual GBD array may assume a configuration different from the one shown through associative and dissociative dislocation reactions, but its effect, insofar as the net relative crystal displacements are concerned, will remain equivalent to that of the array illustrated. This same comment will also apply to all dislocation arrays schematically presented in subsequent figures. Thus each off-coincidence boundary will contain a network of GBD's in which the GBD's delineate regions of the boundary having a structure characterized by the appropriate coincidence pattern. This is identical to the situation in low-angle boundaries, except that in the high-angle case the Burgers vectors of the dislocations are equal to appropriate DSC lattice vectors.

To determine the GBD networks to be found in boundaries of various inclinations, it will prove convenient to utilize the construction of Bishop and Chalmers[26] which considers a grain boundary that changes inclination abruptly from the twist inclination (normal to the rotation axis) to a tilt inclination (parallel to the rotation axis) or some other mixed tilt and twist inclination, as shown schematically in Figure 3. The GBD's present in the twist boundary cannot end within the

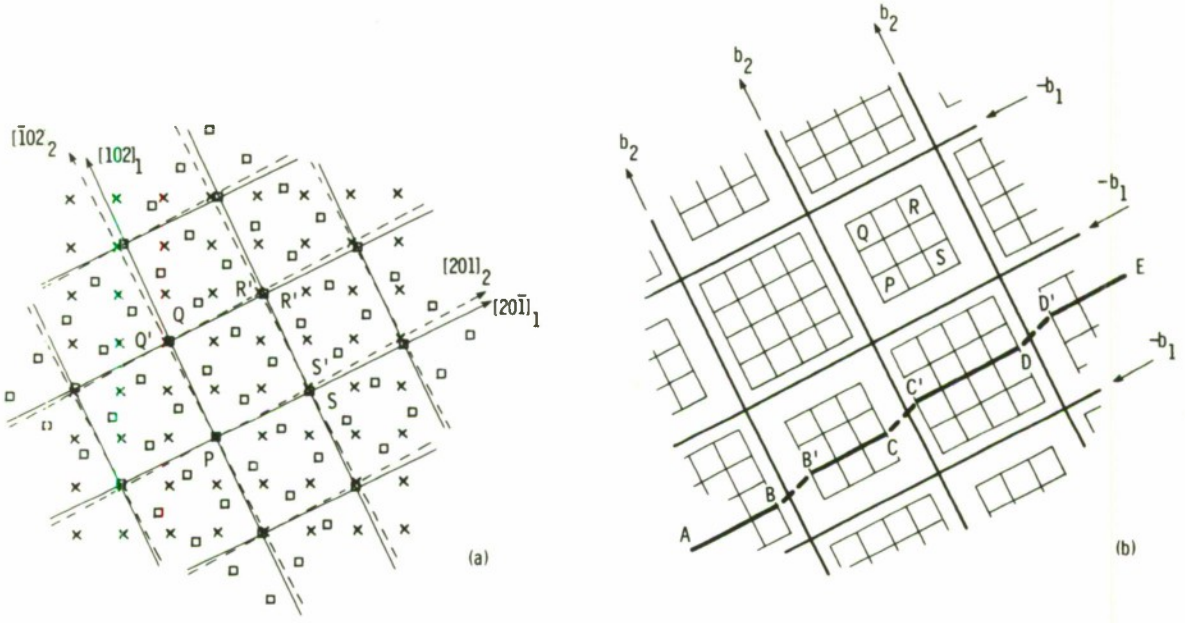

Figure 2. (a) One (010) layer of two interpenetrating simple cubic crystals misoriented by 51.4° about [010]. The slight deviation from the exact coincidence misorientation has caused the former coincidence lattice sites (joined by the solid and dashed lines in the two crystals) to be rotated away from one another. (b) A schematic representation of the grain boundary dislocation array in a twist boundary normal to the [010] rotation axis. The heavy lines are the crossed grid of screw GBD's. The light lines outline the $\Sigma = 5$ coincidence array preserved in the regions between the GBD's, showing the shifting of the pattern in contiguous areas of the boundary. The line AE is the trace of one potential tilt boundary at this misorientation.

crystal and so must be continuous with the GBD's in the boundary in its other inclinations. For example, the crossed network of screw dislocations in the plane ABC in Figure 3a extends onto the plane ABD to give the familiar parallel array of edge dislocations appropriate for the symmetric tilt boundary in that inclination, and onto the plane BCD to give the parallel array of edge dislocations appropriate for the symmetric tilt boundary in that second inclination. Thus, by considering the dislocation content of the twist boundary, the total dislocation content of all other boundaries at that misorientation can be conveniently determined. The value of this construction becomes particularly apparent when the dislocation content of asymmetric tilt boundaries is to be determined, as shown in Figure 3b and as will be our objective later.

THE GBD MODEL — DEVIATIONS FROM NEAR-COINCIDENCE MISORIENTATIONS

Important differences in the GBD model occur when the crystals are noncubic, where it is impossible to establish an exact three-dimensional CSL except under special circumstances. In hexagonal or tetragonal crystals, for example, except for rotations about the c axis, an exact three-dimensional CSL can exist only when $(c/a)^2$ is a rational number, a condition not encountered in any of the common hcp or tetragonal metals at room temperature. In the general case, only near-coincidence-site lattices (near-CSL's) can occur in three dimensions, in which atoms are thought to occupy compromise positions between nearly coincident lattice sites.[27] Corresponding to each near-CSL is an exact CSL which would exist

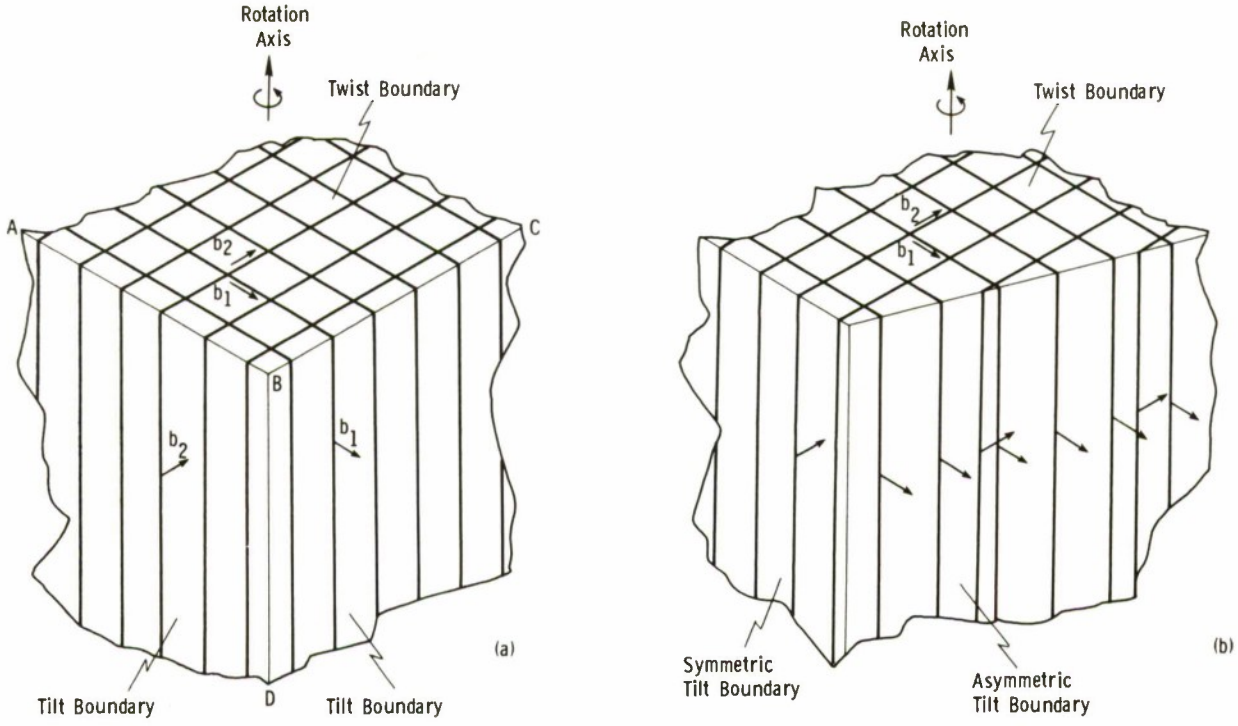

Figure 3. The construction (after Bishop and Chalmers, Ref. 26) showing the transition in grain boundary dislocation structure as the boundary inclination changes from the twist inclination to two possible tilt inclinations, (a) the transition to two symmetric tilt boundaries and (b) the transition to an asymmetric tilt boundary.

at approximately the same misorientation in an ideal crystal with slightly different crystallographic parameters, e.g., one for which $(c/a)^2$ takes on a nearby rational value. The significance of the concept of near-coincidence lies in the fact that coincidence patterns characteristic of the exact CSL in this idealized lattice can be achieved in the real lattice by only small atomic displacements.

It was already discussed in the previous section how deviations from an exact coincidence misorientation led to displacements between former coincidence sites which were locally restored to coincidence by the displacement fields of suitable arrays of GBD's. In the near-coincidence case the displacement fields of the GBD's must restore not only the coincidence lost as a result of a change in misorientation, but also the coincidence lost (actually never attained) as a result of nonideal crystallographic parameters. Thus patterns characteristic of the exact CSL can be achieved in grain boundaries in the vicinity of near-coincidence misorientations by the introduction of suitable GBD's whose displacement fields accomplish the atomic displacements made necessary by both of these factors. In spite of there being an added component of the GBD array resulting from near-coincidence, the Burgers vectors of the total array will be a DSC lattice vector characteristic of the exact CSL.

Consider Figure 4a in which two slightly tetragonal crystals (c/a is slightly greater than one) are misoriented by a rotation of just under 53.1° about [010]. The misorientation has been taken such that an exact two-dimensional CSL exists in the plane formed by the common [010] rotation axis and the line PQ, i.e., the tilt boundary whose trace is PQ is an exact coincidence boundary. Due to the

tetragonality, the exact CSL PQRS of Figure 1 is transformed into a near-CSL in Figure 4a; the former exhibits perfect three-dimensional periodicity whereas the latter does not. At the locations corresponding to the exact coincidence sites R and S in Figure 1, there is only near-coincidence in Figure 4a, i.e., R and R', and S and S' are slightly separated. Furthermore, as the distance increases from the plane of exact coincidence, there is an ever-widening divergence between the rows of atomic sites that locally define the near-CSL, such as those sites along the lines through PS and PS'.

Figure 4a was purposely drawn to closely resemble the coincidence pattern in Figure 1. In fact, the exact coincidence pattern in the plane formed by the common [010] direction and the line PQ is the same in Figures 1 and 4a. In a direction normal to this plane, however, the situation is more like that in Figure 2, in that nearly coincident sites are displaced from one another (e.g., R from R', S from S', etc.) in the same manner that coincidence sites in Figure 1 were displaced from one another by the slight change in misorientation from the exact coincidence misorientation, with the exception that the displacements between near-coincidence sites in Figure 4 *are all in a single direction.* Should the two crystals in Figure 4a be separated by an [010] twist boundary, the same low-energy coincidence pattern, PQRS, characteristic of Figure 1, can be produced by allowing the crystals to shear slightly *in a direction parallel to PQ only,* while localizing the necessary strains in the cores of a single set of GBD's. This is illustrated schematically in Figure 4b, in which only a single set of parallel screw GBD's is necessary to preserve the coincidence pattern. Because the coincidence pattern corresponding to Figure 1 is being preserved, the pertinent pattern-preserving displacements are those defined by the DSC lattice in Figure 1, *even though the crystals in Figure 4 are noncubic and can never achieve this exact coincidence pattern in all three dimensions.*

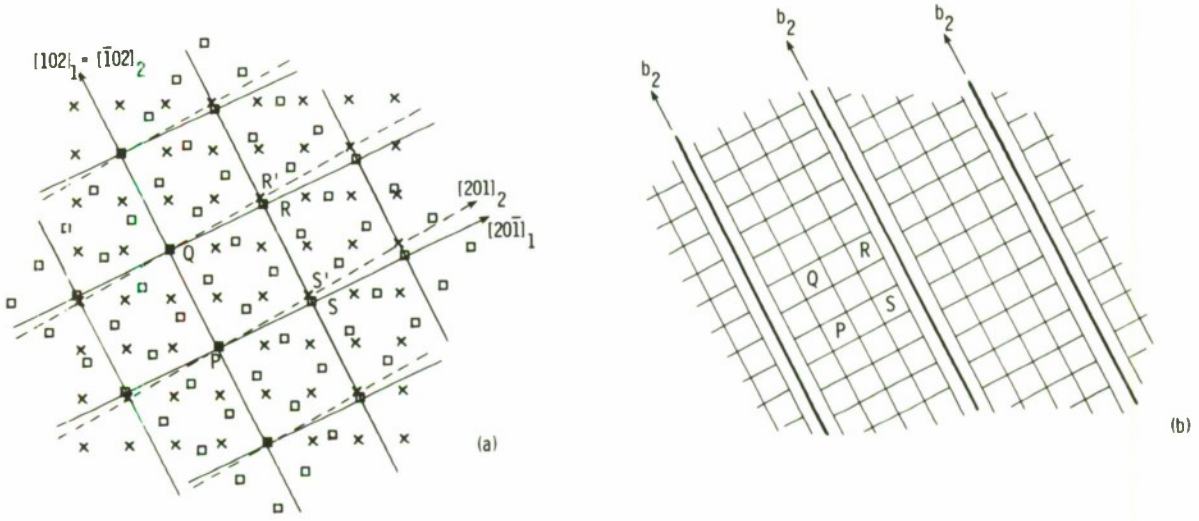

Figure 4. (a) One (010) layer of two interpenetrating slightly tetragonal crystals (c/a = 1.04) misoriented by 51.4° about the common [010]. The solid and dashed lines join sites on what eventually becomes the $\Sigma = 5$ coincidence pattern. Coincidence is exact in the plane defined by the line PQ and the common [010]. Elsewhere near-coincidence or a deviation from coincidence exists. This misorientation is designated θ_1. (b) A schematic representation of the GBD array in the twist boundary normal to [010]. The heavy lines are a single set of screw GBD's separating regions of the boundary in which the $\Sigma = 5$ coincidence pattern (outlined by the lighter lines) is preserved.

An analogous condition prevails at a misorientation in which the rotation about [010] is taken to be slightly greater than 53.1°, as shown in Figure 5a. The situation is reversed in that the plane of exact coincidence is now formed by the common [010] direction and the line PS, with the diverging rows of atomic sites occurring normal to that plane, i.e., along the lines through PQ and PQ', and the displacements between near-coincidence sites are always parallel to PS. The coincidence pattern in the plane of exact coincidence is the same as in the corresponding plane of Figure 1. Once more the low-energy coincidence pattern characteristic of Figure 1 can be retained in the [010] twist boundary by a small elastic shear parallel to PS, again concentrating the mismatch in a single set of parallel screw GBD's separating two such areas. This is illustrated schematically in Figure 5b.

The principle being established here is that departures from exact coincidence due to lower crystallographic symmetry (i.e., in this case, near-coincidence due to noncubicity of the lattice) are completely analogous to departures from exact coincidence due to slight rotations away from the coincidence misorientation, and that in both cases the coincidence pattern is retained by localizing the distortions in the displacement fields of appropriate GBD's. In other words, the exact coincidence pattern retains its same significance in the near-coincidence case, where the deviation is a small crystallographic distortion, as in the off-coincidence case, where the deviation is a small rotation.

The critical point with regard to the Burgers vectors of the GBD's is that the pattern-preserving displacements are those related to the exact coincidence pattern and do not change because of a slight change in crystallography. Whereas the unit vectors b_1 and b_2 of the DSC lattice associated with the coincidence pattern in Figure 1 were both vectors of the type 1/5<102>, they remain vectors of the type 1/5<102> when that pattern is to be preserved in the near-coincidence case.

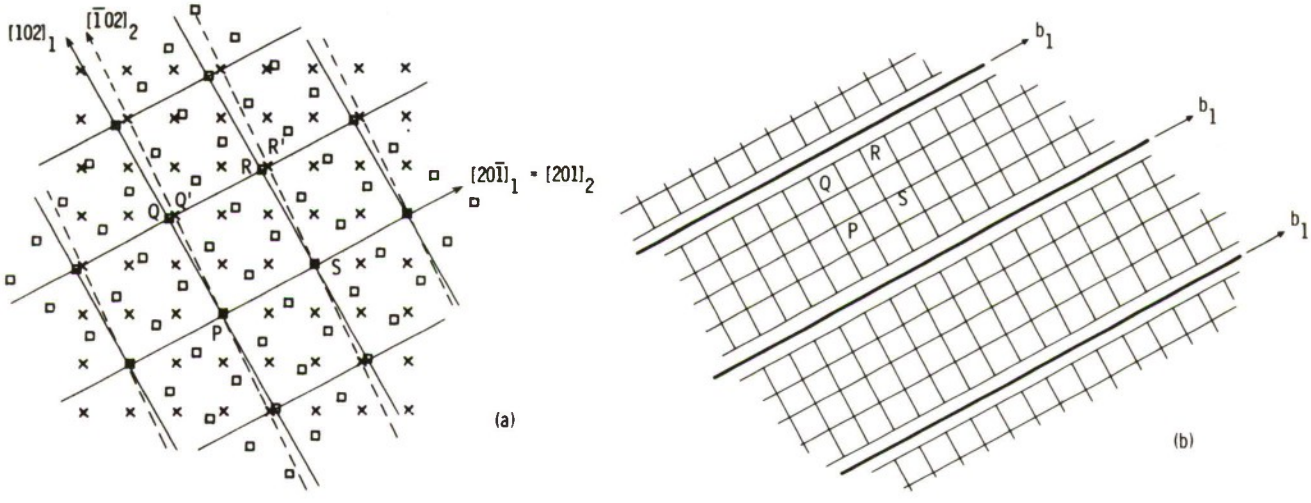

Figure 5. (a) One (010) layer of two interpenetrating slightly tetragonal crystals (c/a = 1.04) misoriented by 54.9° about [010]. The solid and dashed lines join sites on what eventually becomes the $\Sigma = 5$ coincidence pattern. At this misorientation (designated θ_2) coincidence is exact only in the plane defined by the line PS and the common [010]. (b) A schematic representation of the GBD array in the twist boundary normal to [010]. The heavy lines are a single set of screw GBD's separating regions of the boundary in which the $\Sigma = 5$ coincidence pattern (outlined by the lighter lines) is preserved.

Next consider quantitatively the differences between the dislocation structure of a twist grain boundary deviating slightly from an exact coincidence misorientation and one deviating from near-coincidence. Referring to the coincidence pattern of Figure 1 and to the [010] twist boundaries in Figures 2, 4, and 5, these differences may be summarized as follows: If the exact coincidence misorientation corresponding to Figure 1 is θ_o, and the two perpendicular sets of screw dislocations have Burgers vectors b_1 and b_2 as correspondingly shown in Figure 2, then at the off-coincidence misorientation θ the dislocation spacings are

$$d_1 = b_1/(\theta - \theta_o) \tag{1a}$$

and

$$d_2 = b_2/(\theta - \theta_o). \tag{1b}$$

If b_1 and b_2 have equal magnitudes, as was the case here, then $d_1 = d_2$ so that the dislocations form a square grid, as in Figure 2b. The resulting dislocation structures in the two symmetric tilt inclinations represented in Figure 3a, therefore, are both arrays of uniformly spaced edge dislocations of equal spacing, one array having b_1 Burgers vectors, the other b_2 Burgers vectors. Similarly, with near-coincidence, if θ_1 is the misorientation at which coincidence is exact along PQ (cf. Figure 4a) and θ_2 is the misorientation at which coincidence is exact along PS (cf. Figure 5a), and b_2 and b_1 are Burgers vectors parallel to PQ and PS, respectively, then at the nearby misorientation θ the dislocation spacings in the twist boundary are

$$d_1 = b_1/(\theta - \theta_1) \tag{2a}$$

and

$$d_2 = b_2/(\theta - \theta_2). \tag{2b}$$

In Figure 4, $\theta = \theta_1$ so that $d_1 = \infty$ and only a single set of b_2 screw dislocations is required to preserve the coincidence pattern in that twist boundary. Therefore at $\theta = \theta_1$ the tilt boundary along PQ is an exact coincidence boundary; all other tilt boundaries are off-coincidence boundaries and contain a GBD network of edge dislocations having Burgers vectors equal to b_2. In Figure 5, $\theta = \theta_2$ so that $d_2 = \infty$ and only a single set of b_1 screw dislocations is required to preserve the coincidence pattern in that twist boundary. Thus, at $\theta = \theta_2$, the tilt boundary along PS is an exact coincidence boundary and all others are off-coincidence boundaries containing arrays of b_1 edge dislocations.

As the misorientation varies from less than θ_1 to greater than θ_2, a continuous change in dislocation spacing occurs in the twist boundary, as illustrated in Figure 6a. This may be compared to the analogous transition in dislocation structure for the exact coincidence case in Figure 6b, where θ has been varied from below θ_o to above θ_o. The primary difference between the cases deviating from exact coincidence and those deviating from near-coincidence is in the dislocation spacing. In the exact coincidence case, the ratio of the dislocation spacings is equal to the ratio of the lengths of the orthogonal Burgers vectors, i.e., $d_1:d_2 = b_1:b_2$; in the near-coincidence case this is not true, $d_1:d_2 \neq b_1:b_2$. In both cases the pattern-preserving displacements (i.e., the GBD Burgers vectors) are those which preserve the exact coincidence pattern, but each type of dislocation and its spacing must be considered separately in relation to its displacement field and the relative crystal displacements actually encountered at a given misorientation.

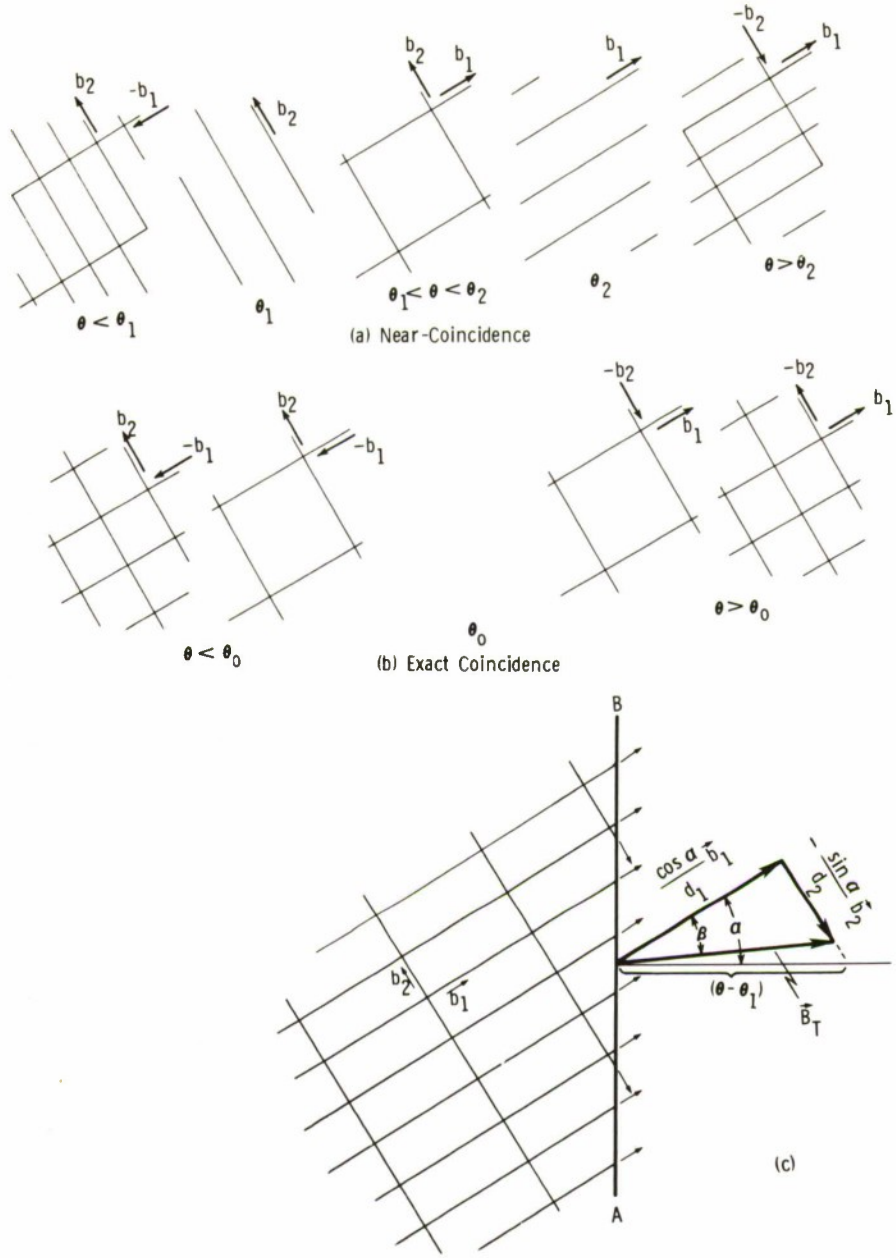

Figure 6. The GBD arrays in twist boundaries of various misorientations, illustrating the relative changes in dislocation spacing. (a) The near-coincidence case (cf. Figures 4 and 5) for misorientations ranging from below θ_1 to above θ_2. (b) The exact coincidence case (cf. Figures 1 and 2) for misorientations ranging from below the exact coincidence misorientation θ_o to above θ_o. (c) A detail taken from Figure 6(a), $\theta > \theta_2$, showing the normalized total Burgers vector in the asymmetric tilt boundary whose trace is AB.

A further difference is encountered in the direction of the normalized total Burgers vector (i.e., the Burgers vector sum per unit length of boundary) in asymmetrically inclined tilt boundaries.* Consider the generally inclined tilt boundary having AB as its trace in Figure 6c, where AB makes an angle α with the

*A distinction will be made between the normalized Burgers vector B and individual Burgers vectors b_i, where in a boundary of unit length $B = \Sigma b_i$. If all dislocations of an array have the same Burgers vector, $B = b/d$.

symmetric inclination parallel to b_2. Let β be the angle between the net Burgers vector per unit length and the normal to the symmetric boundary. It is readily shown that, for θ_1 and θ_2 both close to θ,

$$\tan\beta = (\theta-\theta_2)/(\theta-\theta_1)\ \tan\alpha \tag{3}$$

and

$$|B_T| = (\theta-\theta_1)\ \cos\alpha/\cos\beta = (\theta-\theta_2)\ \sin\alpha/\sin\beta. \tag{4}$$

If $\theta_1 = \theta_2 = \theta_o$ (the exact coincidence case), $\beta = \alpha$ and the net Burgers vector is normal to the boundary, as is also true in all low-angle boundaries. Furthermore,

$$\Delta\theta = (\theta-\theta_o) = |B_T|, \tag{5}$$

the same expression that relates $\Delta\theta$ and B in the familiar low-angle regime applying in high-angle boundaries as well, except that θ is measured relative to the coincidence misorientation.

In the near-coincidence case, however, $\theta_1 \neq \theta_2$; therefore $\beta \neq \alpha$ (except at $\alpha = 0°$ and $\alpha = 90°$) and the net Burgers vector *is not normal to the boundary*. Also $(\theta-\theta_1) \neq |B_T|$, but rather, from Equation 4

$$(\theta-\theta_1) = |B_T|\ \cos\beta/\cos\alpha. \tag{6}$$

The magnitude of $|\theta-\theta_1|$ is therefore given by the b_1 component of B_T projected parallel to b_2 onto the boundary normal, as shown in Figure 6c. The grain boundary shear apparently introduced by B_T not being normal to the boundary in fact exactly compensates the shear distortion generated when a near-coincidence pattern is locally constrained to conform to an exact coincidence pattern in a high-angle tilt boundary. The greater the crystallographic deviation from exact coincidence (i.e., the greater the difference between θ_1 and θ_2), the greater is this shear distortion and the greater must become the component of the normalized total Burgers vector parallel to the boundary plane. This parallel component of the total Burgers vector acts in the same manner as the misfit dislocations in semicoherent interfaces, i.e., they maintain lattice registry across the boundary. However, just as increased strength of the Burgers vector or decreased spacing of the misfit dislocations leads to eventual loss in coherency, similarly, should the required parallel component of the total Burgers vector be too large, as when θ_1 is considerably different than θ_2, the preservation of that particular coincidence pattern becomes incompatible with the large shear distortions, and the boundary structure will assume a configuration unrelated to that pattern.

Notice that it is never possible to form an asymmetric exact coincidence boundary in the near-coincidence case. From Equation 4, except for $\alpha = 0$, $|B_T|$ is always nonzero, and it is impossible for a dislocation-free asymmetric tilt boundary to exist. Even at the special misorientation and special inclination in the range $\theta_1 < \theta < \theta_2$ for which $\alpha-\beta = 90°$, there will be a net Burgers vector lying entirely in the boundary plane, producing a boundary that is completely analogous to a semicoherent or epitaxial interphase interface. Such a grain boundary consists of regions characterized by an asymmetric coincidence pattern interspersed by an array of misfit dislocations. These asymmetric coincidence

patterns are the asymmetric structural units discussed by Bruggeman et al.[27] and by Hartt et al.,[28] and the shear displacements of the misfit array may be identified with the mismatch in structural units which the structural unit model indicated would be accommodated by a suitable array of misfit dislocations. This need for an array of misfit dislocations anticipated by the structural unit model is therefore clearly evident in the GBD model, and in most cases is more easily evaluated in terms of the latter.

A COUPLING OF BOUNDARY MISORIENTATION AND BOUNDARY INCLINATION IN ASYMMETRIC TILT BOUNDARIES

In a generally inclined tilt boundary, it is seldom possible to find a single uniformly spaced array of identical GBD's which have Burgers vectors equal to DSC lattice vectors and which simultaneously allow the resultant normalized total Burgers vector to have the properties specified by Equations 3 and 4. This can usually be accomplished only by the superposition of *two* GBD arrays having two different Burgers vectors. Consequently, a basic assumption of the GBD model of asymmetric tilt boundaries to be presented here is that the normalized total Burgers vector can be resolved into two components: (1) that of a pattern-preserving array B_P, whose function is to preserve the low-energy coincidence pattern, and (2) that of a misfit array B_M, which will be the vector difference between the total Burgers vector and that of the pattern-preserving array. The Burgers vector and spacing of the dislocations of the pattern-preserving array will be selected such that this array alone accounts for the normal component of the total Burgers vector and hence for the change in boundary inclination. The Burgers vector of the misfit array will lie entirely in the boundary plane and so will not influence the misorientation. Neither of these arrays will be stable by itself; each requires the presence of the other to achieve boundary stability.

In considering the GBD's of the pattern-preserving array, it is important to note that while displacements of one crystal relative to the other by lattice vectors of the DSC lattice preserve the coincidence pattern, they also usually cause its position to be shifted in space. For each and every possible GBD Burgers vector there is an associated specific pattern shift. This is true in both the exact coincidence and near-coincidence cases. This shifting of the coincidence pattern on one side of the GBD relative to the other is readily apparent in Figure 2b. For this particular coincidence pattern there are, in fact, five alternative positions into which the pattern can be shifted, reflected by the fact that there are five DSC lattice points within each unit cell of the real crystals, or equivalently that there are five real lattice points of each crystal within the unit cell of the CSL. This number of alternate positions will always equal the coincidence ratio Σ.

The shifting of the coincidence pattern by the GBD's takes on particular significance in the structure of tilt boundaries, in that in most instances the planar coincidence patterns cannot remain coplanar on both sides of the GBD. As a result, the boundary in the tilt inclination will often have to assume a stepped configuration if the same pattern of coincidence sites is to exist on both sides of the GBD, the steps occurring at the positions of the GBD's. For example, the tilt boundary whose trace in Figure 2b starts off along the line AB might be

stepped to the position B'C when one GBD is encountered and then possibly to C'D when the next GBD is encountered, etc. Thus, in order for the grain boundary structure to retain the high density of coincidence sites characteristic of the tilt boundary parallel to PS in Figure 1 (or more correctly the short periodicity of such a coincidence array), it may be advantageous for the boundary to assume a *macroscopic* inclination that is not parallel to PS because of the presence of the GBD's. The asymmetric boundary may then, in some situations, be a lower energy boundary than the symmetric boundary, depending on the balance between the energy associated with the coincidence pattern preserved in the regions between the GBD's and the energy of the GBD array itself.

Figure 7 presents schematically a portion of the dislocation structure of a generally inclined tilt boundary in which steps of magnitude L are associated with each GBD of the pattern-preserving array. Only the pattern-preserving array is represented in the figure. Assuming Crystal 1 to lie to the left of the roughly vertical boundary and Crystal 2 to the right, the Burgers vector of the GBD will define the displacement of Crystal 2 relative to Crystal 1. In addition, the sense of the dislocation line will be taken to be such that an array of edge GBD's with positive Burgers vectors (i.e., whose Burgers vectors point from the boundary into Crystal 2) will tend to increase the misorientation θ. The heavy lines represent the inclination of the low-energy coincidence pattern that is preserved on both sides of the GBD's. The pertinent parameters are defined as follows:

b_p = the Burgers vector of the individual pattern-preserving GBD's
d = the distance between GBD's
L = the distance the coincidence pattern is shifted normal to the plane of the pattern, relative to the unshifted pattern, after Crystal 2 has been displaced by b/2 and Crystal 1 by -b/2.
α = the angle between the normal to the symmetric inclination and the normal to the boundary plane.
α_o = the angle between the normal to the symmetric inclination and the normal to the plane of the low-energy coincidence pattern being preserved.
β = the angle between the normal to the symmetric inclination and the normalized total Burgers vector B_T.
γ = the angle between the normal to the symmetric inclination and the Burgers vector of the pattern-preserving array b_p.
$\Delta\theta = \theta - \theta_1$ = the change in crystal misorientation across the boundary from that at which the symmetric inclination is an exact coincidence boundary.

The normalized Burgers vector of the pattern-preserving array will be selected such that its component normal to the boundary plane is equal to the normal component of the total Burgers vector, leaving a vector difference (B_T-Bp) parallel to the boundary and equal to the Burgers vector B_M of the array of misfit dislocations. From Figure 7b, this is represented by

$$b_p/d \cos(\gamma-\alpha) = |B_T| \cos(\beta-\alpha). \qquad (7)$$

Figure 7b illustrates the case for which $\beta<\alpha$; however, throughout the following discussion the same equations apply for $\beta=\alpha$ and $\beta>\alpha$.

Combining Equation 7 with Equation 4 and noting from Figure 7a that

$$\sin(\alpha-\alpha_o) = L/d, \tag{8}$$

the change in misorientation from that at which the symmetric boundary parallel to b_2 is exactly coincident may be written

$$\Delta\theta = \theta-\theta_1 = \frac{b_p \cos(\gamma-\alpha) \sin(\alpha-\alpha_o) \cos\beta}{L \cos(\beta-\alpha) \cos\alpha}. \tag{9}$$

For $\beta = \alpha$ (the exact coincidence case) this reduces to

$$\theta-\theta_1 = \frac{b_p \cos(\gamma-\alpha) \sin(\alpha-\alpha_o)}{L}. \tag{10}$$

Thus, for a change in θ, there is a uniquely defined coupled change in the boundary inclination α determined by the magnitude and direction of the Burgers vector and the associated pattern shift which it produces.

The relationship between boundary misorientation θ and boundary inclination α can be obtained by an iterative process, using Equation 10 as an initial approximation, solving for θ at a given α, determining β from Equation 3, and recalculating θ from Equation 9. The final two steps may be repeated until convergence

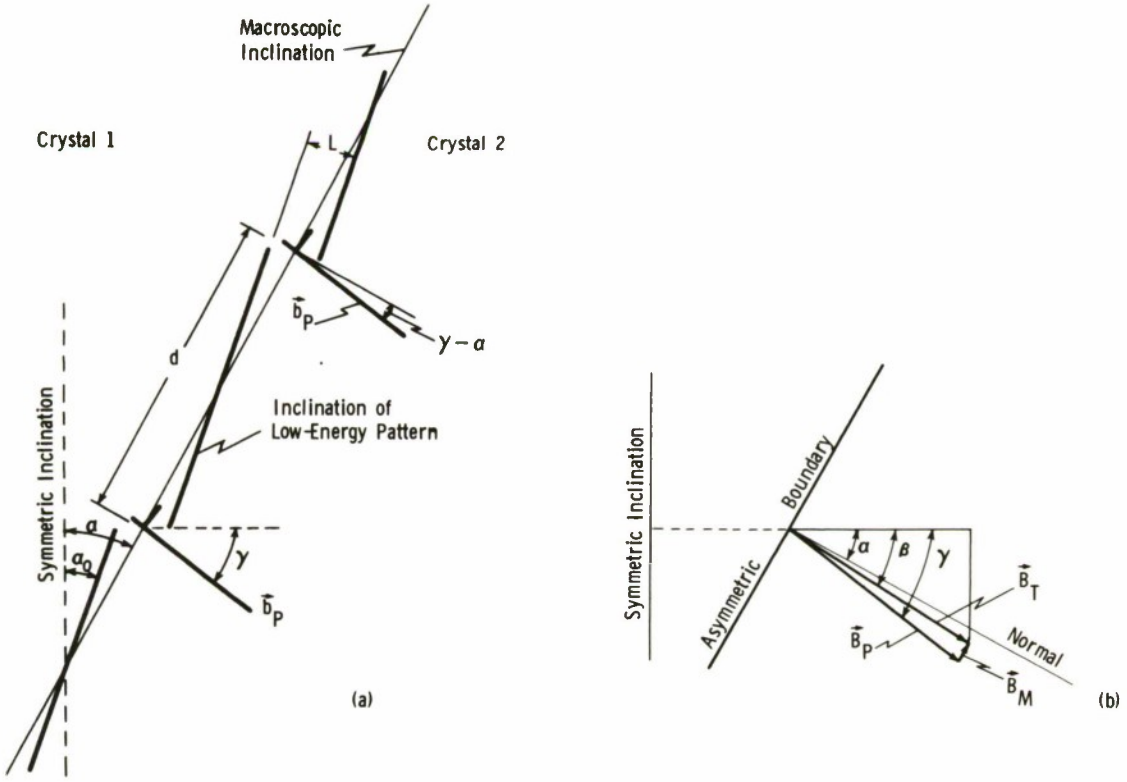

Figure 7. (a) A generally inclined tilt boundary consisting of regions characterized by a low-energy coincidence pattern separated by tilt GBD's of the pattern-preserving array. (b) A diagram showing the relationship between the normalized total Burgers vector B_T, the normalized pattern-preserving Burgers vector B_P, and the normalized misfit Burgers vector B_M in the asymmetric boundary in (a).

is achieved. Because θ_1 will normally be close to θ_2, β is nearly equal to α (except in a small angular range on either side of θ_1 and θ_2) so that the calculation converges rapidly.

Again referring to Figure 7b, it can be shown that the magnitude of the normalized Burgers vector of the misfit array is given by

$$|B_M| = \left|(\theta-\theta_1)\ \frac{\sin(\beta-\gamma)\ \cos\alpha}{\cos(\alpha-\gamma)\ \cos\beta}\right| = \left|(\theta-\theta_2)\ \frac{\sin(\beta-\gamma)\ \sin\alpha}{\cos(\alpha-\gamma)\ \sin\beta}\right|. \qquad (11)$$

Only when $\beta = \gamma$ is the array of misfit dislocations unnecessary for boundary stability, i.e., when the normalized pattern-preserving Burgers vector equals the normalized total Burgers vector. At the other extreme, when $\alpha-\beta = 90°$, the total Burgers vector lies entirely in the boundary plane, and Equation 11 then reduces to Equation 4 to give

$$|B_M| = |B_T|. \qquad (12)$$

It is tacitly assumed that, in low-energy boundaries, $|B_M|$ will be small allowing the misfit dislocations to be widely spaced, causing the misfit array to have an insignificant effect on the boundary energy and morphology relative to the influence of the low-energy coincidence pattern and the pattern-preserving dislocation array. Thus, the model assumes that the boundary structure is controlled predominantly by the pattern-preserving array, an assumption justified experimentally.

The energy of the pattern-preserving GBD array will include both the contribution of the long-range strain field of the GBD's and of their core energies. The long-range contribution will be a function of the size of the Burgers vector of the GBD's (and, in tilt boundaries, of the Burgers vector component parallel to the boundary). From this standpoint GBD's having small Burgers vectors with no parallel component will be favored in tilt boundaries. The core energy contribution will reflect the disturbances in bond energies experienced by those atoms lying in the core regions of the GBD's. When a boundary step is associated with the GBD, the structure of the step can be viewed as the core structure of the GBD and hence will determine the core energy of the dislocation. Good-fitting steps, i.e., steps in which atomic separations and atomic coordination are disturbed as little as possible from that of the bulk crystal, undoubtedly minimize the core energy. This condition will turn out to be most readily achieved when the lattice displacement produced by the GBD causes only a small pattern shift, allowing the step to be small and enabling the core region of the GBD to resemble, in the cases examined thus far, a unit of a low-energy short-period coincidence boundary. This latter detail will be amply illustrated in Part II. Such details aside, the general expectations regarding the minimization of the core energy are that short steps exhibiting good atomic fit will be energetically favored.

The optimum boundary structure at a given misorientation, i.e., the boundary of lowest energy, must strike a balance between all of the factors previously discussed. The requirements placed upon the Burgers vectors of the pattern-preserving GBD's may be summarized as follows: (a) they must be DSC lattice vectors; (b) they should be short to minimize the long-range strain energy; (c) they should lead to short, good-fitting steps in the boundary to minimize the GBD core energy; and

(d) in the case of near-coincidence they should be as closely normal to the boundary plane as possible, thereby reflecting a minimum in the shear distortion intrinsic to near-coincidence. It would appear from data to be presented elsewhere that the core energy contribution exercises dominant influence over the boundary structure, at least in asymmetric tilt boundaries. The boundary inclination will depend on the size of the steps caused by the GBD's and the spacing between steps (i.e., the dislocation spacing), both of these factors being dictated by the Burgers vector and the latter also by the misorientation. As the boundary misorientation deviates more and more from that at which the coincidence pattern is most nearly exact, greater and greater numbers of grain boundary dislocations are incorporated into the boundary structure where they not only accommodate the small changes in misorientation but also can produce a definite and systematic change in the boundary inclination.

The misfit dislocation array adds to the total boundary energy and so mitigates the energy reduction effected by the preservation of the low-energy coincidence pattern. Nevertheless, it is the preservation of the coincidence pattern which apparently exercises dominant influence on the boundary energy and the boundary structure, and it is for this reason that application of the model in the subsequent paper will focus primarily on the pattern-preserving array.

The above model has here been presented from the standpoint that the dislocation structure of the boundary will determine its morphology, and that low-energy GBD arrays lead to low-energy boundary inclinations. While this is true for equilibrium boundary configurations, the *cause* and *effect* roles are more likely reversed for the majority of high-angle grain boundaries encountered experimentally, since the boundary inclination is often determined by nonequilibrium factors. In this case the boundary inclination determines what the dislocation structure of the boundary must be at a given boundary misorientation to assure crystallographic compatibility across the interface. Nevertheless, both points of view are represented in the same relationships between boundary misorientation, boundary inclination, and boundary structure, in which specification of two of these elements automatically determines the third.

SUMMARY

The application of the grain boundary dislocation model to boundary structure in noncubic crystals is shown to require some important changes from the GBD model applied to cubic crystals. More specifically, these variations are encountered when conditions of exact coincidence cannot be crystallographically achieved but rather only conditions of near-coincidence. The low-energy coincidence patterns associated with exact coincidence can be preserved in the near-coincidence case, but only at the expense of an inherent shear distortion at the interface. The lattice displacements or GBD Burgers vectors that preserve these coincidence patterns are defined by the DSC lattice derived for the exact coincidence relationship.

The shear distortion that occurs when a near-coincidence pattern is locally constrained to conform to an exact coincidence pattern gives rise to some unusual features in the dislocation structure of the boundary. In twist boundaries

deviating from an exact coincidence misorientation, the two orthogonal shears that produce the relative crystal rotation at the interface are equal (i.e., $d_1b_1 = d_2b_2$); in the near-coincidence case they are not (i.e., $d_1b_1 \neq d_2b_2$). In fact, at certain misorientations one shear or the other may be totally absent. In asymmetric tilt boundaries the total Burgers vector is not normal to the interface, as it always is in the exact coincidence case, thereby compensating for the shear distortion due to near-coincidence.

The total dislocation content of a tilt grain boundary can be resolved into two components: (1) a pattern-preserving array of GBD's, whose function is to preserve the low-energy coincidence pattern on either side of the GBD while minimizing primarily the dislocation core contribution to the boundary energy, and (2) an array of misfit dislocations, whose function is to compensate for any interfacial shear introduced by the pattern-preserving array. Finally, the pattern-preserving array appears to exercise dominant influence over boundary energy and morphology, in that boundary steps can be associated with each pattern-preserving GBD, thereby producing a systematic, experimentally verifiable coupled change in boundary inclination with boundary misorientation.

LITERATURE CITED

1. BOLLMANN, W., and NISSEN, H.-U. *A Study of Optimal Phase Boundaries: The Case of Exsolved Alkali Feldspars.* Acta Cryst., v. 24A, 1968, p. 546-557.
2. GLEITER, H., HORNBOGEN, E., and BARO, G. *The Mechanism of Grain Boundary Glide.* Acta Met., v. 16, 1968, p. 1053-1067.
3. ISHIDA, Y., HASEGAWA, T., and NAGATA, F. *Grain-Boundary Fine Structure in an Iron Alloy.* J. Appl. Phys., v. 40, 1969, p. 2182-2186.
4. LEVY, J. *The Structure of High-Angle Grain Boundaries in Aluminum.* Phys. Stat. Sol., v. 31, 1969, p. 193-201.
5. SCHOBER, T., and BALLUFFI, R. W. *Dislocation Subboundary Arrays in Oriented Thin-Film Bicrystals.* Phil. Mag., v. 20, 1969, p. 511-518.
6. GLEITER, H. *The Mechanism of Grain Boundary Migration.* Acta Met., v. 17, 1969, p. 565-573.
7. SCHOBER, T., and BALLUFFI, R. W. *Quantitative Observation of Misfit Dislocation Arrays in Low and High-Angle Twist Grain Boundaries.* Phil. Mag., v. 21, 1970, p. 109-123.
8. SCHOBER, T. *Observation of Misfit Dislocation Arrays in High Angle (110) Twist Grain Boundaries in Gold.* Phil. Mag., v. 22, 1970, p. 1063-1068.
9. SCHOBER, T., and BALLUFFI, R. W. *Extraneous Grain Boundary Dislocations in Low and High Angle (001) Twist Boundaries in Gold.* Phil. Mag., v. 24, 1971, p. 165-180.
10. SCHOBER, T., and BALLUFFI, R. W. *Observation of Dislocation Arrays in Low Angle Tilt Boundaries in Gold.* Phys. Stat. Sol. (b), v. 44, 1971, p. 103-114.
11. SCHOBER, T., and BALLUFFI, R. W. *Dislocations in Symmetric High Angle [001] Tilt Boundaries in Gold.* Phys. Stat. Sol. (b), v. 44, 1971, p. 115-126.
12. BUZZICHELLI, G., and MASCANZONI, A. *On the Generation and Motion of Grain Boundary Dislocations in Steel.* Phil. Mag., v. 24, 1971, p. 497-508.
13. BALLUFFI, R. W., WOOLHOUSE, G. R., and KOMEN, Y. *On Grain Boundary Dislocation Contrast in the Electron Microscope* in The Nature and Behavior of Grain Boundaries, H. Hu, ed., Plenum Press, 1972, p. 41.
14. BALLUFFI, R. W., KOMEN, Y., and SCHOBER, T. *Electron Microscope Studies of Grain Boundary Dislocation Behavior.* Surface Science, v. 31, 1972, p. 68-103.
15. MIEKK-OJA, H. M., and LINDROOS, V. K. *The Formation of Dislocation Networks.* Surface Science, v. 31, 1972, p. 422-455.
16. SCHOBER, T., and WARRINGTON, D. H. *Extraneous Grain Boundary Dislocations in High Angle (110) Twist Boundaries in Gold.* Phys. Stat. Sol. (a), v. 6, 1971, p. 103-110.
17. BALLUFFI, R. W., SASS, S. L., and SCHOBER, T. *Grain Boundary Dislocation Networks as Electron Diffraction Gratings.* Phil. Mag., v. 26, 1972, p. 585-592.
18. LOBERG, B., and NORDEN, H. *Regular Defect Structures in High Angle Grain Boundaries.* Acta Met., v. 21, 1973, p. 213-218.
19. KEGG, G. R., HORTON, C. A. P., and SILCOCK, J. M. *Grain Boundary Dislocations in Aluminum Bicrystals After High-Temperature Deformation.* Phil. Mag., v. 27, no. 5, May 1973, p. 1041-1055.
20. McDONALD, R. C., and ARDELL, A. J. *On Diffraction Contrast Effects at Extrinsic Grain Boundary Dislocations.* Phys. Stat. Sol. (a), v. 18, 1973, p. 407-417.
21. BRANDON, D. G., RALPH, B., RANGANATHAN, S., and WALD, M. S. *A Field Ion Microscope Study of Atomic Configuration at Grain Boundaries.* Acta Met., v. 12, 1964, p. 813-821.
22. BRANDON, D. G. *The Structure of High-Angle Grain Boundaries.* Acta Met., v. 14, 1966, p. 1479-1484.
23. BISHOP, G. H., and CHALMERS, B. *A Coincidence-Ledge-Dislocation Description of Grain Boundaries.* Scripta Met., v. 2, 1968, p. 133-140.
24. BOLLMANN, W. *Crystal Defects and Crystalline Interfaces.* Springer-Verlag, 1970, p. 148.
25. HIRTH, J. P., and BALLUFFI, R. W. *On Grain Boundary Dislocations and Ledges.* Acta Met., v. 21, 1973, p. 929-942.
26. BISHOP, G. H., and CHALMERS, B. *Dislocation Structure and Contrast in High-Angle Grain Boundaries.* Phil. Mag., v. 24, 1971, p. 515-526.
27. BRUGGEMAN, G. A., BISHOP, G. H., and HARTT, W. H. *Coincidence and Near-Coincidence Grain Boundaries in HCP Metals* in The Nature and Behavior of Grain Boundaries, H. Hu, ed., Plenum Press, 1972, p. 83.
28. HARTT, W. H., BISHOP, G. H., and BRUGGEMAN, G. A. *Grain Boundary Faceting of $\langle 10\bar{1}0 \rangle$ Tilt Boundaries in Zinc – Part II.* Acta Met., v. 22, 1974, p. 971-983.
29. BISHOP, G. H., HARTT, W. H., and BRUGGEMAN, G. A. *Grain Boundary Faceting of $\langle 10\bar{1}0 \rangle$ Tilt Boundaries in Zinc.* Acta Met., v. 19, 1971, p. 37-47.

TECHNICAL REPORT DISTRIBUTION

No. of Copies	To
1	Office of the Director, Defense Research and Engineering, The Pentagon, Washington, D. C. 20301
12	Commander, Defense Documentation Center, Cameron Station, Building 5, 5010 Duke Street, Alexandria, Virginia 22314
1	Metals and Ceramics Information Center, Battelle Memorial Institute, 505 King Avenue, Columbus, Ohio 43201
1	Chemical Propulsion Information Agency, Applied Physics Laboratory, The Johns Hopkins University, 8621 Georgia Avenue, Silver Spring, Maryland 20910
	Chief of Research and Development, Department of the Army, Washington, D. C. 20310
2	ATTN: Physical and Engineering Sciences Division
	Commander, Army Research Office, P. O. Box 12211, Research Triangle Park, North Carolina 27709
1	ATTN: Information Processing Office
	Commander, U. S. Army Materiel Development and Readiness Command, 5001 Eisenhower Avenue, Alexandria, Virginia 22333
1	ATTN: DRCDE-TC
1	DRCSA-S, Dr. R. B. Dillaway, Chief Scientist
	Commander, U. S. Army Electronics Command, Fort Monmouth, New Jersey 07703
1	ATTN: DRSEL-GG-DD
1	DRSEL-GG-DM
	Commander, U. S. Army Missile Command, Redstone Arsenal, Alabama 35809
1	ATTN: Technical Library
1	DRSMI-RSM, Mr. E. J. Wheelahan
	Commander, U. S. Army Armament Command, Rock Island, Illinois 61201
2	ATTN: Technical Library
	Commander, U. S. Army Natick Laboratories, Natick, Massachusetts 01760
1	ATTN: Technical Library
	Commander, U. S. Army Satellite Communications Agency, Fort Monmouth, New Jersey 07703
1	ATTN: Technical Document Center
	Commander, U. S. Army Tank-Automotive Development Center, Warren, Michigan 48090
2	ATTN: DROTA, Research Library Branch
	Commander, White Sands Missile Range, New Mexico 88002
1	ATTN: STEWS-WS-VT
	Commander, Aberdeen Proving Ground, Maryland 21005
1	ATTN: STEAP-TL, Bldg. 305
	President, Airborne, Electronics and Special Warfare Board, Fort Bragg, North Carolina 28307
1	ATTN: Library
	Commander, Dugway Proving Ground, Dugway, Utah 84022
1	ATTN: Technical Library, Technical Information Division
	Commander, Edgewood Arsenal, Maryland 21010
1	ATTN: Mr. F. E. Thompson, Dir. of Eng. & Ind. Serv., Chem-Mun Br
	Commander, Frankford Arsenal, Philadelphia, Pennsylvania 19137
1	ATTN: Library, H1300, Bl. 51-2
1	SMUFA-L300, Mr. J. Corrie
	Commander, Harry Diamond Laboratories, 2800 Powder Mill Road, Adelphi, Maryland 20783
1	ATTN: Technical Information Office
	Commander, Picatinny Arsenal, Dover, New Jersey 07801
1	ATTN: SMUPA-RT-S
	Commander, Redstone Scientific Information Center, U. S. Army Missile Command, Redstone Arsenal, Alabama 35809
4	ATTN: DRSMI-RBLD, Document Section
	Commander, Watervliet Arsenal, Watervliet, New York 12189
1	ATTN: SARWV-RDT, Technical Information Services Office
	Commander, U. S. Army Foreign Science and Technology Center, 220 7th Street, N. E., Charlottesville, Virginia 22901
1	ATTN: DRXST-SD3
	Director, Eustis Directorate, U. S. Army Air Mobility Research and Development Laboratory, Fort Eustis, Virginia 23604
1	ATTN: Mr. J. Robinson, SAVDL-EU-SS
	Librarian, U. S. Army Aviation School Library, Fort Rucker, Alabama 36360
1	ATTN: Building 5907
	Commander, U. S. Army Engineer School, Fort Belvoir, Virginia 22060
1	ATTN: Library
	Commandant, U. S. Army Quartermaster School, Fort Lee, Virginia 23801
1	ATTN: Quartermaster School Library
	Naval Research Laboratory, Washington, D. C. 20375
1	ATTN: Dr. J. M. Krafft - Code 8430
2	Dr. G. R. Yoder - Code 6382
	Chief of Naval Research, Arlington, Virginia 22217
1	ATTN: Code 471
	Air Force Materials Laboratory, Wright-Patterson Air Force Base, Ohio 45433
2	ATTN: AFML (MXE), E. Morrissey
1	AFML (LC)
1	AFML (LMD), D. M. Forney
1	AFML (MBC), S. Schulman
	National Aeronautics and Space Administration, Washington, D. C. 20546
1	ATTN: Mr. B. G. Achhammer
1	Mr. G. C. Deutsch - Code RR-1
	National Aeronautics and Space Administration, Marshall Space Flight Center, Huntsville, Alabama 35812
1	ATTN: R-P&VE-M, R. J. Schwinghamer
1	S&E-ME-MM, Mr. W. A. Wilson, Building 4720
1	Ship Research Committee, Maritime Transportation Research Board, National Research Council, 2101 Constitution Ave., N. W., Washington, D. C. 20418
	P. R. Mallory Company, Inc., 3029 East Washington Street, Indianapolis, Indiana 46206
1	ATTN: Technical Library
	Wyman-Gordon Company, Worcester, Massachusetts 01601
1	ATTN: Technical Library
1	The Charles Stark Draper Laboratory, 68 Albany Street, Cambridge, Massachusetts 02139
1	Materials Sciences Corporation, Blue Bell Campus, Merion Towle Bldg., Blue Bell, Pennsylvania 19422
	Director, Army Materials and Mechanics Research Center, Watertown, Massachusetts 02172
2	ATTN: DRXMR-PL
1	DRXMR-AG
2	Authors

Army Materials and Mechanics Research Center,
Watertown, Massachusetts 02172
GRAIN BOUNDARY DISLOCATIONS IN NONCUBIC
CRYSTALS – I. THE MODEL –
Gordon A. Bruggeman and George H. Bishop, Jr.

Technical Report AMMRC TR 76-6, March 1976, 21 pp –
illustrations, D/A Project 1T161102B32A,
AMCMS Code 611102.11.85500

AD _____

UNCLASSIFIED
UNLIMITED DISTRIBUTION

Key Words

Grain boundaries
Crystallography
Dislocations

A model is developed for the dislocation structure of grain boundaries in noncubic crystals. Important differences are noted between the grain boundary dislocation (GBD) description of boundaries in cubic and noncubic crystals. In both types of crystals the GBD's are present to preserve low-energy patterns characteristic of exact coincidence-site lattices (CSL's). In cubic crystals exact three-dimensional CSL's can be found for rotations about any axis. In noncubic crystals, however, exact three-dimensional CSL's exist only in special circumstances; in general, only near-coincidence site lattices (near-CSL's) can occur in three dimensions. When only near-coincidence is possible an additional component to the GBD array is necessary to compensate for the distortion implicit in near-coincidence. In twist boundaries this additional component alters the spacing of dislocations in the screw grid. Moreover, it is impossible to obtain a twist boundary free of GBD's. The minimum dislocation content occurs at misorientations at which exact coincidence exists in a single plane parallel to the twist axis, i.e., when an exact two-dimensional CSL exists, in which case a single set of screw GBD's parallel to the plane of exact coincidence is present. In tilt boundaries two dislocation arrays may be necessary: an array of pattern-preserving dislocations and an array of misfit dislocations. The function of the former array is to preserve the low-energy coincidence pattern on either side of the GBD; the function of the misfit array is again to compensate for the distortion inherent in near-coincidence. The pattern-preserving GBD's are shown to introduce steps in tilt grain boundaries, altering the boundary inclination as the dislocation content of the boundary varies. As a result, a systematic, experimentally verifiable coupled change in boundary inclination with boundary misorientation is predicted for each potential pattern-preserving GBD.

Army Materials and Mechanics Research Center,
Watertown, Massachusetts 02172
GRAIN BOUNDARY DISLOCATIONS IN NONCUBIC
CRYSTALS – I. THE MODEL –
Gordon A. Bruggeman and George H. Bishop, Jr.

Technical Report AMMRC TR 76-6, March 1976, 21 pp –
illustrations, D/A Project 1T161102B32A,
AMCMS Code 611102.11.85500

AD _____

UNCLASSIFIED
UNLIMITED DISTRIBUTION

Key Words

Grain boundaries
Crystallography
Dislocations

A model is developed for the dislocation structure of grain boundaries in noncubic crystals. Important differences are noted between the grain boundary dislocation (GBD) description of boundaries in cubic and noncubic crystals. In both types of crystals the GBD's are present to preserve low-energy patterns characteristic of exact coincidence-site lattices (CSL's). In cubic crystals exact three-dimensional CSL's can be found for rotations about any axis. In noncubic crystals, however, exact three-dimensional CSL's exist only in special circumstances; in general, only near-coincidence site lattices (near-CSL's) can occur in three dimensions. When only near-coincidence is possible an additional component to the GBD array is necessary to compensate for the distortion implicit in near-coincidence. In twist boundaries this additional component alters the spacing of dislocations in the screw grid. Moreover, it is impossible to obtain a twist boundary free of GBD's. The minimum dislocation content occurs at misorientations at which exact coincidence exists in a single plane parallel to the twist axis, i.e., when an exact two-dimensional CSL exists, in which case a single set of screw GBD's parallel to the plane of exact coincidence is present. In tilt boundaries two dislocation arrays may be necessary: an array of pattern-preserving dislocations and an array of misfit dislocations. The function of the former array is to preserve the low-energy coincidence pattern on either side of the GBD; the function of the misfit array is again to compensate for the distortion inherent in near-coincidence. The pattern-preserving GBD's are shown to introduce steps in tilt grain boundaries, altering the boundary inclination as the dislocation content of the boundary varies. As a result, a systematic, experimentally verifiable coupled change in boundary inclination with boundary misorientation is predicted for each potential pattern-preserving GBD.

Army Materials and Mechanics Research Center,
Watertown, Massachusetts 02172
GRAIN BOUNDARY DISLOCATIONS IN NONCUBIC
CRYSTALS – I. THE MODEL –
Gordon A. Bruggeman and George H. Bishop, Jr.

Technical Report AMMRC TR 76-6, March 1976, 21 pp –
illustrations, D/A Project 1T161102B32A,
AMCMS Code 611102.11.85500

AD _____

UNCLASSIFIED
UNLIMITED DISTRIBUTION

Key Words

Grain boundaries
Crystallography
Dislocations

A model is developed for the dislocation structure of grain boundaries in noncubic crystals. Important differences are noted between the grain boundary dislocation (GBD) description of boundaries in cubic and noncubic crystals. In both types of crystals the GBD's are present to preserve low-energy patterns characteristic of exact coincidence-site lattices (CSL's). In cubic crystals exact three-dimensional CSL's can be found for rotations about any axis. In noncubic crystals, however, exact three-dimensional CSL's exist only in special circumstances; in general, only near-coincidence site lattices (near-CSL's) can occur in three dimensions. When only near-coincidence is possible an additional component to the GBD array is necessary to compensate for the distortion implicit in near-coincidence. In twist boundaries this additional component alters the spacing of dislocations in the screw grid. Moreover, it is impossible to obtain a twist boundary free of GBD's. The minimum dislocation content occurs at misorientations at which exact coincidence exists in a single plane parallel to the twist axis, i.e., when an exact two-dimensional CSL exists, in which case a single set of screw GBD's parallel to the plane of exact coincidence is present. In tilt boundaries two dislocation arrays may be necessary: an array of pattern-preserving dislocations and an array of misfit dislocations. The function of the former array is to preserve the low-energy coincidence pattern on either side of the GBD; the function of the misfit array is again to compensate for the distortion inherent in near-coincidence. The pattern-preserving GBD's are shown to introduce steps in tilt grain boundaries, altering the boundary inclination as the dislocation content of the boundary varies. As a result, a systematic, experimentally verifiable coupled change in boundary inclination with boundary misorientation is predicted for each potential pattern-preserving GBD.

Army Materials and Mechanics Research Center,
Watertown, Massachusetts 02172
GRAIN BOUNDARY DISLOCATIONS IN NONCUBIC
CRYSTALS — I. THE MODEL —
Gordon A. Bruggeman and George H. Bishop, Jr.

Technical Report AMMRC TR 76-6, March 1976, 21 pp — illustrations, D/A Project 1T161102B32A, AMCMS Code 611102.11.85500

AD _____

UNCLASSIFIED
UNLIMITED DISTRIBUTION

Key Words

Grain boundaries
Crystallography
Dislocations

A model is developed for the dislocation structure of grain boundaries in noncubic crystals. Important differences are noted between the grain boundary dislocation (GBD) description of boundaries in cubic and noncubic crystals. In both types of crystals the GBD's are present to preserve low-energy patterns characteristic of exact coincidence-site lattices (CSL's). In cubic crystals exact three-dimensional CSL's can be found for rotations about any axis. In noncubic crystals, however, exact three-dimensional CSL's exist only in special circumstances; in general, only near-coincidence site lattices (near-CSL's) can occur in three dimensions. When only near-coincidence is possible an additional component to the GBD array is necessary to compensate for the distortion implicit in near-coincidence. In twist boundaries this additional component alters the spacing of dislocations in the screw grid. Moreover, it is impossible to obtain a twist boundary free of GBD's. The minimum dislocation content occurs at misorientations at which exact coincidence exists in a single plane parallel to the twist axis, i.e., when an exact two-dimensional CSL exists, in which case a single set of screw GBD's parallel to the plane of exact coincidence is present. In tilt boundaries two dislocation arrays may be necessary: an array of pattern-preserving dislocations and an array of misfit dislocations. The function of the former array is to preserve the low-energy coincidence pattern on either side of the GBD; the function of the misfit array is again to compensate for the distortion inherent in near-coincidence. The pattern-preserving GBD's are shown to introduce steps in tilt grain boundaries, altering the boundary inclination as the dislocation content of the boundary varies. As a result, a systematic, experimentally verifiable coupled change in boundary inclination with boundary misorientation is predicted for each potential pattern-preserving GBD.

Army Materials and Mechanics Research Center,
Watertown, Massachusetts 02172
GRAIN BOUNDARY DISLOCATIONS IN NONCUBIC
CRYSTALS — I. THE MODEL —
Gordon A. Bruggeman and George H. Bishop, Jr.

Technical Report AMMRC TR 76-6, March 1976, 21 pp — illustrations, D/A Project 1T161102B32A, AMCMS Code 611102.11.85500

AD _____

UNCLASSIFIED
UNLIMITED DISTRIBUTION

Key Words

Grain boundaries
Crystallography
Dislocations

A model is developed for the dislocation structure of grain boundaries in noncubic crystals. Important differences are noted between the grain boundary dislocation (GBD) description of boundaries in cubic and noncubic crystals. In both types of crystals the GBD's are present to preserve low-energy patterns characteristic of exact coincidence-site lattices (CSL's). In cubic crystals exact three-dimensional CSL's can be found for rotations about any axis. In noncubic crystals, however, exact three-dimensional CSL's exist only in special circumstances; in general, only near-coincidence site lattices (near-CSL's) can occur in three dimensions. When only near-coincidence is possible an additional component to the GBD array is necessary to compensate for the distortion implicit in near-coincidence. In twist boundaries this additional component alters the spacing of dislocations in the screw grid. Moreover, it is impossible to obtain a twist boundary free of GBD's. The minimum dislocation content occurs at misorientations at which exact coincidence exists in a single plane parallel to the twist axis, i.e., when an exact two-dimensional CSL exists, in which case a single set of screw GBD's parallel to the plane of exact coincidence is present. In tilt boundaries two dislocation arrays may be necessary: an array of pattern-preserving dislocations and an array of misfit dislocations. The function of the former array is to preserve the low-energy coincidence pattern on either side of the GBD; the function of the misfit array is again to compensate for the distortion inherent in near-coincidence. The pattern-preserving GBD's are shown to introduce steps in tilt grain boundaries, altering the boundary inclination as the dislocation content of the boundary varies. As a result, a systematic, experimentally verifiable coupled change in boundary inclination with boundary misorientation is predicted for each potential pattern-preserving GBD.

Army Materials and Mechanics Research Center,
Watertown, Massachusetts 02172
GRAIN BOUNDARY DISLOCATIONS IN NONCUBIC
CRYSTALS — I. THE MODEL —
Gordon A. Bruggeman and George H. Bishop, Jr.

Technical Report AMMRC TR 76-6, March 1976, 21 pp — illustrations, D/A Project 1T161102B32A, AMCMS Code 611102.11.85500

AD _____

UNCLASSIFIED
UNLIMITED DISTRIBUTION

Key Words

Grain boundaries
Crystallography
Dislocations

A model is developed for the dislocation structure of grain boundaries in noncubic crystals. Important differences are noted between the grain boundary dislocation (GBD) description of boundaries in cubic and noncubic crystals. In both types of crystals the GBD's are present to preserve low-energy patterns characteristic of exact coincidence-site lattices (CSL's). In cubic crystals exact three-dimensional CSL's can be found for rotations about any axis. In noncubic crystals, however, exact three-dimensional CSL's exist only in special circumstances; in general, only near-coincidence site lattices (near-CSL's) can occur in three dimensions. When only near-coincidence is possible an additional component to the GBD array is necessary to compensate for the distortion implicit in near-coincidence. In twist boundaries this additional component alters the spacing of dislocations in the screw grid. Moreover, it is impossible to obtain a twist boundary free of GBD's. The minimum dislocation content occurs at misorientations at which exact coincidence exists in a single plane parallel to the twist axis, i.e., when an exact two-dimensional CSL exists, in which case a single set of screw GBD's parallel to the plane of exact coincidence is present. In tilt boundaries two dislocation arrays may be necessary: an array of pattern-preserving dislocations and an array of misfit dislocations. The function of the former array is to preserve the low-energy coincidence pattern on either side of the GBD; the function of the misfit array is again to compensate for the distortion inherent in near-coincidence. The pattern-preserving GBD's are shown to introduce steps in tilt grain boundaries, altering the boundary inclination as the dislocation content of the boundary varies. As a result, a systematic, experimentally verifiable coupled change in boundary inclination with boundary misorientation is predicted for each potential pattern-preserving GBD.